ChemComm

Accepted Manuscript

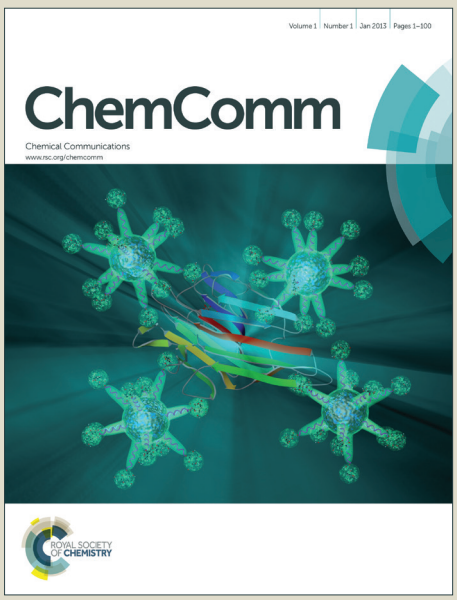

This is an *Accepted Manuscript*, which has been through the Royal Society of Chemistry peer review process and has been accepted for publication.

Accepted Manuscripts are published online shortly after acceptance, before technical editing, formatting and proof reading. Using this free service, authors can make their results available to the community, in citable form, before we publish the edited article. We will replace this *Accepted Manuscript* with the edited and formatted *Advance Article* as soon as it is available.

You can find more information about *Accepted Manuscripts* in the Information for Authors.

Please note that technical editing may introduce minor changes to the text and/or graphics, which may alter content. The journal's standard Terms & Conditions and the Ethical guidelines still apply. In no event shall the Royal Society of Chemistry be held responsible for any errors or omissions in this *Accepted Manuscript* or any consequences arising from the use of any information it contains.

ROYAL SOCIETY OF CHEMISTRY

www.rsc.org/chemcomm

Chem Comm

RSCPublishing

COMMUNICATION

Silicon carbide coated with TiO_2 with enhancing cobalt active phase dispersion for Fischer-Tropsch synthesis

Cite this: DOI: 10.1039/x0xx00000x

Yuefeng Liu,*[a] Ileana Florea,[b] Ovidiu Ersen,[b] Cuong Pham-Huu*[a] and Christian Meny[b]

Received 00th January 2012,
Accepted 00th January 2012

DOI: 10.1039/x0xx00000x

www.rsc.org/

The introduction of a thin layer of TiO_2 on β-SiC allows a significant improvement of the cobalt dispersion. This catalyst exhibits an excellent and stable catalytic activity for the Fishcher-Tropsch synthesis (FTS) with high C_{5+} selectivity, which contributes to the development of new active catalysts family in the gas-to-liquid process.

Fischer-Tropsch synthesis (FTS), which converts synthesis gas (a mixture of CO and H_2) derived from coal, natural gas (also shale gas) or biomass, into synthetic liquid fuels and chemicals, continues to attract more interests as a result of diminishing petroleum reserves and a seek for clean fuel.[1-3] The FTS reaction is strongly exothermic,[4-7] i.e. ΔH = -204 $kJmol^{-1}_{CO}$ and thus, a large amount of heat was generated during the course of the reaction. In the case of insulator supports, the heat generated on the catalyst surface leads to the formation of local hot spots on the catalyst surface which significantly affects the overall selectivity towards liquid hydrocarbons production.

Silicon carbide (β-SiC) has been recently reported to be an efficient support for fixed-bed FTS reaction due to its intrinsic medium thermal conductivity which facilitate heat dissipation throughout the catalyst body and thus, avoided the formation of local hot spots which are detrimental for the liquid hydrocarbons selectivity.[8-11] The large porosity of the support also allows a rapid escaping of the intermediate liquid hydrocarbons and water and thus, significantly contributes to the improvement of the liquid hydrocarbon selectivity as well.[12] However, the metal-support interaction between the cobalt phase and the SiC surface is relatively weak, leading to the formation of medium to large cobalt particles which are less efficient for the FTS reaction. In our previous attempts to improve SiC-based catalyst performance for the FTS reaction, the SiC surface was modified by introducing dopant which exhibits a higher metal-support interaction in order to achieve the better dispersion of the deposited cobalt phase.[10] However, on such composite support some large cobalt particles remaining in contact with SiC phase which could lower the overall FTS performance of the catalyst.[11, 13] It is of interest to develop new doping method to homogeneously decorate the SiC surface with a thin layer of TiO_2 in order to efficiently disperse the cobalt particles which in turn, improves the FTS performance. It is expected that the future development of the FTS requires the introduction of active and stable catalysts. Herein, we report on the development of a highly active and stable FTS catalyst based on titania coated (TS-Cx where x is the TiO_2 weight percent) high porosity industrial β-SiC containing well dispersed cobalt particles. The high dispersion of the cobalt particles on the thin TiO_2 layer leads to a significant improvement of the catalyst activity for the FTS reaction compared to the undoped SiC and TiO_2 doped SiC (TS-D) catalysts. According to our best knowledge, the FTS activity of this SiC-based catalyst is the most active one among the different cobalt-based catalysts, either pure or doped with trace amount of noble metal.

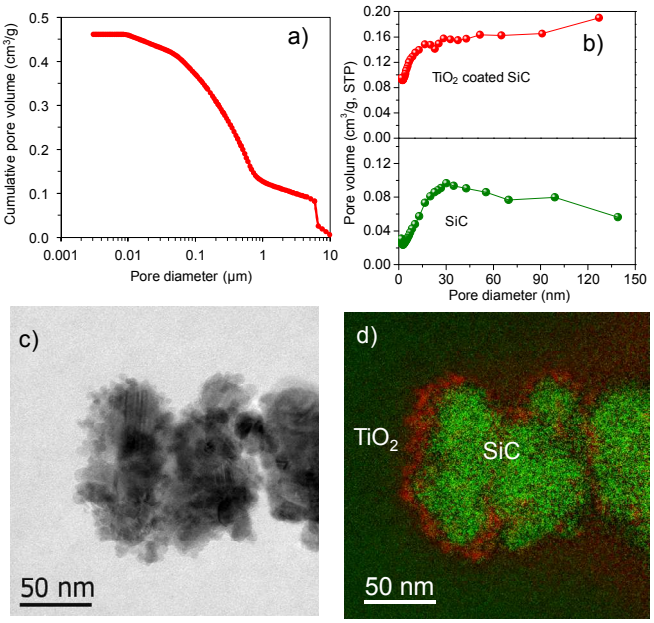

Fig. 1 Characterization of the TiO_2 coated SiC (TS-C10) support. (a) Pore size distributions measured by mercury intrusion of the TiO_2 coated SiC composite, (b) Pore size distribution by BJH method of the SiC and TiO_2 coated SiC. (c) 2D TEM image of TiO_2 coated SiC and (d) corresponding EFTEM image of the classical 2D TEM map which clearly shows the well distribution of TiO_2 on the topmost

ChemComm Accepted Manuscript

surface of SiC. (TiO_2 (red), SiC (green)).

The SiC is mostly consisting of large amount of meso-, and macropores (Figure 1a). The transformation of the titanium precursor, deposited through an incipient wetness method on the SiC surface, into TiO_2 crystalline phase is performed by calcination of the sample in air at 600 °C for 5 h. The obtained TiO_2 layer is well crystallized in a single anatase phase as confirmed by XRD and XPS analysis (Figures S1 and S2, ESI†).[14, 15] The specific surface area (S_{BET}) of the TiO_2 coated SiC is in the range of 39-41m^2/g (Tabel S1, ESI†), which is close to the pure SiC (40 m^2/g). Such results could be attributed to the meso-and macropore of the support which contributes to the homogeneous coating of the TiO_2 layer on the SiC surface. The pore size distribution curves in the range of 2 -150 nm derived from adsorption branches of the N_2 isotherms using BJH method is presented in Figure 1b. TiO_2 coated SiC and SiC supports display irregular and broad pore size distribution which is different from those reported for SiO_2 and Al_2O_3 supports.[16, 17] The TEM and energy filtered TEM (EFTEM) of the TiO_2 coated SiC composite presented in Figure 1c and d clearly show the presence of a thin and homogeneous TiO_2 layer covering the surface of the SiC support. The similar trends of morphologies and elemental distribution (Figure S3, ESI†) confirm the homogeneous coating of the support. The specific surface area of the catalyst, after depositing 10 wt. % of cobalt, is remains unchanged (ca. 40 m^2/g) (Table 1) which indicate that the cobalt phase is relatively well dispersed on the support surface and no pore plugging is encountered.

Table 1. Characteristis and FTS performance of SiC and TiO_2-SiC supported cobalt catalysts.[a]

Sample	S_{BET} (m^2/g)	V_{total} (cm^3/g)	d_{Co}^0 (nm)[b]	X_{CO} (%)	Sel. (%)				CoTY[c]	α[d]
					CH_4	CO_2	C_{2-4}	C_{5+}		
10CS[e]	33	0.14	20	32.3	4.5	0	2.4	93.1	4.8	0.92
10CTS-D[e][f]	25	0.08	18	43.4	4.5	0	1.9	93.6	6.5	0.92
10CTS-C10[g]	40	0.11	10	61.0	5.8	0.1	2.9	91.2	12.1	0.91

[a] All data were collected after 20 h time-on stream with stable catalytic performance. Reaction conditions: Co loading = 10 wt. %, H_2/CO = 2, 225 °C, 40 bar. [b] Particle size was calculated based on the ^{59}Co NMR results of the cobalt atoms fraction engaged in the different blocking temperature ranges. [c] Cobalt Time Yield (CoTY, 10^{-5} $mol_{co}\cdot g_{Co}^{-1}s^{-1}$, molar CO conversion rate per gram of Co per hour). [d] Chain growth probability factor (α). [e] 10CS: 10 wt % of cobalt on SiC; 10CTS-D: 10 wt % of cobalt on SiC doped with TiO_2 (with 17 wt% loading), gas velocity of 60 $mL\cdot g_{cat}^{-1}\cdot min^{-1}$. [f] SiC doped with TiO_2 supported catalyst, data from ref.[10]. [g] SiC coated with TiO_2 supported catalyst (10 wt% of cobalt on SiC coated with 10 wt% TiO_2). Gas velocity of 80 $mL\cdot g_{cat}^{-1}\cdot min^{-1}$

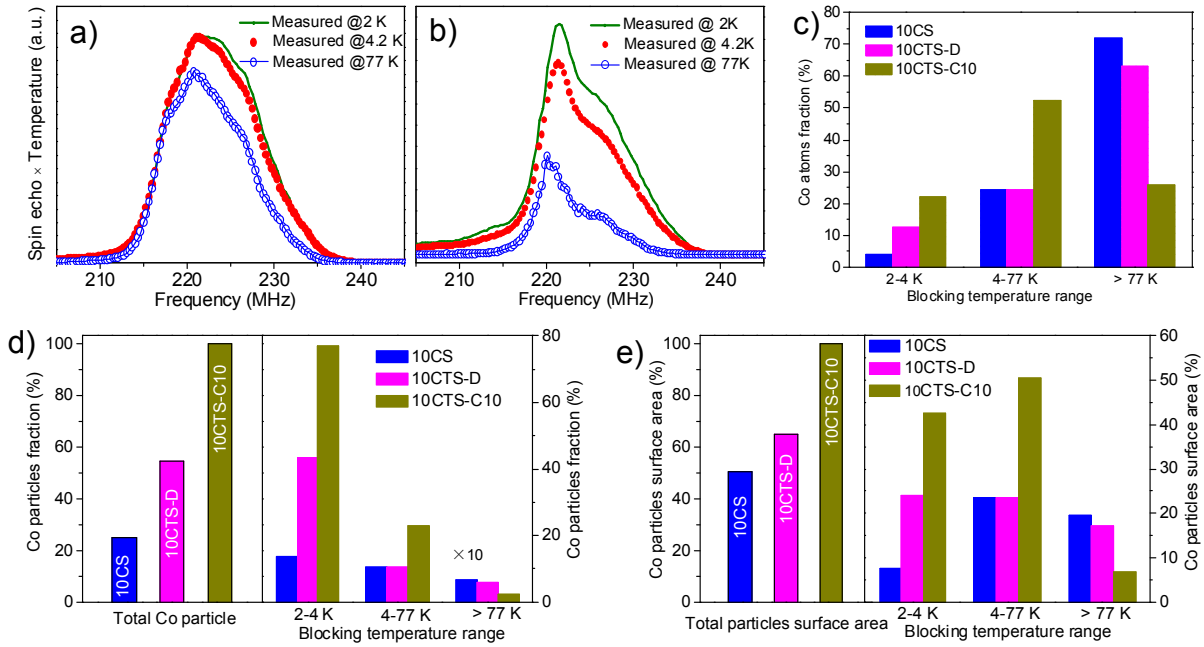

Fig. 2 ^{59}Co NMR spectra of the (a) 10CS and (b) 10CTS-C10 catalysts after FTS test covered with solid wax. Recorded temperatures are 2, 4.2 and 77K. (c) Co fraction atoms engaged in the different blocking temperature ranges (size ranges). (d) Total number of cobalt particles (left panel) and distribution of cobalt particles as a function of the blocking temperature (right panel) produced in the samples. (e) Total Co particles surface area (left panel) and the relative particles surface area as a function of the blocking temperature ranges (right panel). The data in (d) and (e) are normalized to the sample showing the largest available number of particles and surface area (assuming the same initial atomic cobalt content), respectively.

ChemComm Accepted Manuscript

This journal is © The Royal Society of Chemistry 2012

Journal Name RSCPublishing

COMMUNICATION

The TEM and the corresponding energy-dispersive X-ray spectroscopy (EDX) spectra of 10CoTS-C10 in different areas of the sample are presented in Figure S4 (ESI†). The EDX spectra reveal that cobalt and titanium are localized in the same area, confirming the fact that cobalt is well dispersed on the surface of TiO_2. Next, nil field spin-echo ^{59}Co NMR is performed to understand the relationship between the structures of active sites and FTS activity. Figures 2a and b show the ^{59}Co NMR spectra recorded on the cobalt supported on SiC (10CS) and TiO_2 coated SiC (10CTS-C10) at 3 different temperatures. A significant contribution can be observed at 217 MHz in the NMR spectrum of the 10CS catalyst, showing the presence of a large number of Co atoms forming large face centered cubic (fcc) particles with a size larger than 60 nm.[9, 10, 18, 19] Such contribution is not observed in Figure 2b showing that the Co particles are significantly smaller in the presence of TiO_2 coated catalyst. From the temperature dependent NMR spectra, the fraction of cobalt atoms with different blocking temperature ranges (equivalent to different size ranges), as well as the relative percentage of cobalt nanoparticles (Co NPs) sizes and surface area, are presented in Figures 2c-e. On the other hand, on the 10CTS-C10 catalyst, 74 % of cobalt atoms are engaged in the smallest cobalt particles (< 10 nm, blocking temperature 2-4.2 K and 4.2-77K), which is significantly higher than that of 10CS (28 %) and 10CTS-D (37 %) catalysts. It is expected that the high FTS performance (Table 1) obtained on this TiO_2-coated catalyst is directly linked with the presence of small cobalt particles in strong interaction with the TiO_2 coating layer.[20, 21] The average crystallite size of the cobalt is about 20 nm for the 10CS, and about 10 nm for the 10CTS-C10 (Table 1), the later being predicted to be the most active particle size for the FTS process (see discussion below).[22] According to such result one can state that the introduction of the TiO_2 phase onto the SiC matrix significantly decreases the particle size of cobalt, probably by generating a higher chemical interaction with the metal salt precursor without modifying the reduction behavior of the sample. Such evidence is also found in the carbon-based supported cobalt catalyst.[23]

The 10CS (cobalt on SiC), 10CTS-D (cobalt on SiC doped with TiO_2) and 10CTS-C10 (10 wt. % cobalt on SiC coated with 10 wt. % TiO_2) catalysts have been tested in FTS reaction, and the catalytic results are listed in Table 1. The doping or coating of SiC leads to a considerable improvement of the FTS performance compared to that of un-doped one (Table 1). The CO conversion increases from 32.3% to 61.0% after coating a layer of TiO_2 (10 wt. %) on the SiC support. The increase of the FTS catalytic activity is only accompanied by a slight decrease of selectivity for liquid hydrocarbons (C_{5+} selectivity of 10CTS-C catalyst remains as high as 91%). The selectivity of CO_2 for the tested catalysts is less than 0.2% (Table 1). It could be concluded that the water-gas shift reaction is not side reaction over such cobalt-based catalysts. The carbon balance of the different experiments is > 90 ± 4 wt %, which can be ascribed to the difference between the theoretical and experimental carbon balance with the error margin of the CO outlet flow rate and the liquid and solid hydrocarbons recovery. The relatively low carbon balance in the present work is due to the lost of the C_6-C_8 fractions (estimated to about 5 wt. %) during the heating of the trap according to our previous works. It is thus expected that the C_{5+} selectivity will be even higher than the one reported if all the C_6-C_8 fractions are included in the calculation. The chain growth factor (α) determined on various tested catalysts (Table 1) which is calculated by using the Anderson-Schulz-Flory (ASF) model,[3] is relatively high on the TiO_2 coated SiC catalysts (0.91).

The different TiO_2 mass loading (from 0 to 15 wt%) is also investigated, and results (Figures S5 and S6, ESI†) show that the FTS rate increases significantly with the increasing TiO_2 from 0 to 10 wt%. However, the FTS rate goes down when the TiO_2 mass loading is up to 15 wt% which could be attributed to the stronger metal-support interaction between the TiO_2 and the cobalt precursor as the thicker TiO_2 layer is introduced (XRD results in the Figure S5, ESI†). It is also worthy to note that the catalyst exhibits a relatively high stability and no deactivation was observed under the operated reaction conditions.

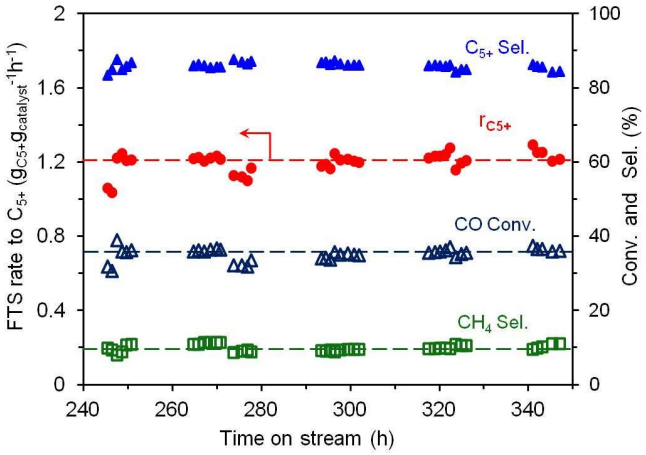

Fig. 3 FTS rate and products selectivity as a function of time on stream on the 30CTS-C10 sample. The catalyst has already been tested in the FTS reaction under different conditions during 240 h on stream before performing this rest.

Moreover, one should expect that the FTS activity is mostly related to the amount of exposed cobalt surface area rather than to the distribution of cobalt atoms. It is known that surface cobalt active sites (atoms surface area) are most probably activating the reaction by direct contact with the reactant molecules. As can be seen in Figure 2e, the 10CTS-D catalyst for example contains 60% of cobalt atoms forming large particles (measured blocking temperature higher than 77 K with particle diameter ranging from 10 nm to 30 nm or even more) but they only represent less than 2% in term of particles fraction, or only offer less than 20 % of the total atoms surface (active sites). It means that small particles (< 10 nm) play the key effects for FTS activity improvement. In the 10CTS-C10 catalyst, about 80% of cobalt atoms formed > 90 % of the fraction of the particles in the range of 3-4 nm and 4-10 nm, which contribute for more than 90% to the particles surface area (3-4 nm and 4-10 nm offered 43% and 50 % of atoms surface area fraction). According to our NMR results, we speculate that the small particles (3-10 nm) have multiple active sites depending on the preparation and materials used as support and are directly involved in the improvement of the FTS catalytic performance.[24] These results are different from the

ChemComm Accepted Manuscript

results reported previously on cobalt supported on carbon nanofibers where low FTS activity is observed when the cobalt NPs size is smaller than 10 nm [21, 22, 25] The peculiar interactions between the cobalt particles and the prismatic planes of the CNFs could be advanced to explain such discrepancy.

We also run the experiment using the cobalt loading up to 30 wt. % under the realistic FTS reaction conditions (240 ^{o}C, 40 bar, and at a relatively high space velocity of 320 $mL \cdot g_{cat}^{-1} \cdot min^{-1}$). According to the results the thermal conductor TiO_2-SiC-based catalyst exhibits a high and stable FTS performance for about 100 h on stream (Figure 3). The specific rate is about 1.22 $g_{C5+} \cdot g_{catalyst}^{-1} \cdot h^{-1}$ with a relatively high C_{5+} selectivity, i.e. 85.8 % and high chain-growth factor (Table S2 and Figure S7, ESI†), which confirms the potential industrial interest of this catalyst in the FTS reaction.

In conclusion, the introduction of a thin coated layer of TiO_2 on the SiC surface significantly improves the metal-support interaction between the cobalt precursor and the support leading to a better dispersion of the cobalt active phase. The catalysts, either with low (10 wt %) or high (30 wt %) cobalt loading, exhibit a high and stable FTS activity and long chain hydrocarbons selectivity along with a long-term stability. The high dispersion of the deposited cobalt particles leading to the formation of small cobalt particles is advanced to explain the high FTS performance of the catalyst while the medium thermal conductivity of the support is expected to be at the origin of a high C_{5+} selectivity even at a relatively high reaction temperature. The meso- and macroporosity of the support is also responsible for the long-term stability of the catalyst by reducing the problem of pore plugging by liquid hydrocarbons produced during the reaction. The combination of the catalytic and the NMR results allow us to clearly evidence a direct relationship between the cobalt particle size and the FTS performance. It is expected that this catalyst could significantly promote the development of the FTS in the near future where the supply of high quality liquid fuels becomes the core process in several sectors.

The authors would like to thank SICAT Co. (www.sicatcatalyst.com) for offer SiC materials. Y.F. Liu thanks the grant from China Scholarship Council (CSC). F. Vigneron, T. Romero and P. Bernhardt are gratefully acknowledged for experimental assistance and SEM/XPS analysis.

Notes and references

[a] Institut de Chimie et Procédés pour l'Energie, l'Environnement et la Santé (ICPEES), UMR 7515, CNRS-University of Strasbourg (UdS), 25, rue Becquerel, 67087 Strasbourg Cedex 02, France
yuefeng.liu@unistra.fr (Y.F. Liu);
cuong.pham-huu@unistra.fr (C. Pham-Huu).
[b] Institut de Physique et Chimie des Matériaux de Strasbourg (IPCMS), UMR 7504, CNRS-University of Strasbourg (UdS), 23, rue du Loess, 67037 Strasbourg Cedex 02, France

†Electronic Supplementary Information (ESI) available: Experimental details and characterizations such as XRD, XPS, SEM-EDX, TEM-EDX and FTS results (Figures S1-S7 and Tables S1-S2) See DOI: 10.1039/c000000x/

1. J. R. Rostrup-Nielsen, *Science*, 2005, **308**, 1421-1422.
2. G. M. Whitesides and G. W. Crabtree, *Science*, 2007, **315**, 796-798.
3. H. M. T. Galvis, J. H. Bitter, C. B. Khare, M. Ruitenbeek, A. I. Dugulan and K. P. de Jong, *Science*, 2012, **335**, 835-838.
4. A. Y. Khodakov, W. Chu and P. Fongarland, *Chemical Reviews*, 2007, **107**, 1692-1744.
5. E. Iglesia, *Appl Catal A-Gen*, 1997, **161**, 59-78.
6. E. de Smit and B. M. Weckhuysen, *Chem Soc Rev*, 2008, **37**, 2758-2781.
7. Q. Zhang, J. Kang and Y. Wang, *ChemCatChem*, 2010, **2**, 1030-1058.
8. A. R. de la Osa, A. De Lucas, J. Diaz-Maroto, A. Romero, J. L. Valverde and P. Sanchez, *Catal Today*, 2012, **187**, 173-182.
9. B. de Tymowski, Y. F. Liu, C. Meny, C. Lefevre, D. Begin, P. Nguyen, C. Pham, D. Edouard, F. Luck and C. Pham-Huu, *Appl Catal A-Gen*, 2012, **419**, 31-40.
10. Y. Liu, B. de Tymowski, F. Vigneron, I. Florea, O. Ersen, C. Meny, P. Nguyen, C. Pham, F. Luck and C. Pham-Huu, *ACS Catalysis*, 2013, **3**, 393-404.
11. Y. Liu, O. Ersen, C. Meny, F. Luck and C. Pham-Huu, *ChemSusChem*, 2014, **7**, 1218-1239.
12. J. Kang, K. Cheng, L. Zhang, Q. Zhang, J. Ding, W. Hua, Y. Lou, Q. Zhai and Y. Wang, *Angew Chem Int Ed*, 2011, **50**, 5200-5203.
13. I. Florea, Y. F. Liu, O. Ersen, C. Meny and C. Pham-Huu, *ChemCatChem*, 2013, **5**, 2610-2620.
14. H. G. Yang, C. H. Sun, S. Z. Qiao, J. Zou, G. Liu, S. C. Smith, H. M. Cheng and G. Q. Lu, *Nature*, 2008, **453**, 638-U634.
15. Y. Wang, H. J. Sun, S. J. Tan, H. Feng, Z. W. Cheng, J. Zhao, A. D. Zhao, B. Wang, Y. Luo, J. L. Yang and J. G. Hou, *Nat Commun*, 2013, **4**.
16. J. P. Hong, W. Chu, P. A. Chernavskii and A. Y. Khodakov, *Appl Catal A-Gen*, 2010, **382**, 28-35.
17. O. Borg, S. Erib, E. A. Blekkan, S. Storsaeter, H. Wigum, E. Rytter and A. Holmen, *J Catal*, 2007, **248**, 89-100.
18. C. Meny and P. Panissod, ed. G. A. Webb, Springer, Heidelberg, Germany 2006.
19. P. Panissod and C. Meny, *Appl Magn Reson*, 2000, **19**, 447-460.
20. W. Chu, L. N. Wang, P. A. Chernavskii and A. Y. Khodakov, *Angew Chem Int Ed*, 2008, **47**, 5052-5055.
21. J. P. den Breejen, P. B. Radstake, G. L. Bezemer, J. H. Bitter, V. Froseth, A. Holmen and K. P. de Jong, *J Am Chem Soc*, 2009, **131**, 7197-7203.
22. G. L. Bezemer, J. H. Bitter, H. P. C. E. Kuipers, H. Oosterbeek, J. E. Holewijn, X. D. Xu, F. Kapteijn, A. J. van Dillen and K. P. de Jong, *J Am Chem Soc*, 2006, **128**, 3956-3964.
23. Y. Liu, J. Luo, M. Girleanu, O. Ersen, C. Pham-Huu and C. Meny, *J Catal*, 2014, **318**, 179-192.
24. Z. J. Wang, S. Skiles, F. Yang, Z. Yan and D. W. Goodman, *Catal Today*, 2012, **181**, 75-81.
25. G. Prieto, A. Martinez, P. Concepcion and R. Moreno-Tost, *J Catal*, 2009, **266**, 129-144.

ChemComm Accepted Manuscript

 This journal is © The Royal Society of Chemistry 2012